Design of a practical optical cross-connect with limited-range wavelength conversion

Zichun Le (乐孜纯)[1*], Zhijun Zhu (朱智俊)[1,2], Minglei Fu (付明磊)[1], and Jun Chen (陈　君)[1]

[1]*College of Sciences, Zhejiang University of Technology, Hangzhou 310023, China*

[2]*College of Information Engineering, Zhejiang University of Technology, Hangzhou 310023, China*

[*]*E-mail: lzc@zjut.edu.cn*

Received May 11, 2010

The architecture of and the corresponding control algorithm for a devised optical cross-connect, limited-range wavelength converision wavelength interchangeable cross-connect (L-WIXC), are presented. The performances of L-WIXC including blocking probability, switching time, and throughput are simulated. Cost comparison with wavelength selective cross-connect (WSXC) and WIXC is calculated. Key optical parameters, such as crosstalk, eye diagram, bit error rate, and linear Q factor, are measured and discussed.

OCIS codes: 060.4259, 060.4253, 060.6719.

doi: 10.3788/COL20100812.1120.

A fundamental issue for optical cross-connect (OXC) is how to offer efficient and cost-effective transport services for a wide range of bandwidth granularities, such as waveband, wavelength, and subwavelength[1,2]. Both architecture and blocking probability models for OXC have recently been demonstrated[1−7]. OXC can be divided into three types according to wavelength conversion: wavelength selective cross-connect (WSXC), which does not have wavelength conversion capability, wavelength interchangeable cross-connect (WIXC), which has full wavelength conversion capacity, and limited-range wavelength conversion WIXC (L-WIXC), which has partial wavelength conversion ability[8]. In this letter, a L-WIXC is devised for sub-wavelength switching to support optical burst switching (OBS) in terms of feasibility and reliability. Both the architecture and procedures of the just-in-time (JIT) based control algorithm are given. The blocking probability and cost of the devised L-WIXC are also compared with that of WSXC and WIXC. Moreover, optical parameters, such as channel crosstalk, eye diagram, and linear Q factor, are measured and evaluated.

Figure 1 shows the architectures of WSXC, WIXC, and L-WIXC. The architecture of the devised L-WIXC (Fig. 1(c)) is composed of three demultiplexers at the input ports, three multiplexers at the output ports, five 4×4 optical switches (S1 − S5), and four arbitrary-input fixed-output wavelength converters (WCs) (λ_0 − λ_3). In addition, 4×4 optical switches are controlled by a field programmable gate array (FPGA). Demultiplexed wavelengths are switched to the output ports using the 4×4 optical switches according to the destination address if the corresponding wavelengths are free. If the corresponding wavelengths have been reserved or used and the adjacent wavelengths are free, the wavelength is first switched to S5 and converted to free wavelength. The converted wavelength is then switched to the corresponding output port. Therefore, input wavelengths have two possible switching paths (SPs) in the devised L-WIXC. In the first SP, wavelengths are transmitted through one 4×4 optical switch without wavelength conversion (denoted by SP1). In the other SP, wavelengths must be transmitted from the input optical switch (e.g., S1) to S5 and then sent back to S1 after wavelength conversion (denoted by SP2). The maximum switching time of the 4×4 optical switches is assumed to be 8 ms. Thus, for the burst data packet (BDP) transmitted along SP1, the maximum switching time is 8 ms. For the BDP transmitted along SP2, the maximum switching time is 24 ms.

To test the performance of the L-WIXC, a test bed was built under the circumstance of the OBS network (Fig. 2). BDPs transferred into the optical signals using a distributed feedback laser diode (DFB-LD) were coupled into the fiber using a multiplexer. Burst control packets (BCPs) were transmitted to the FPGA control

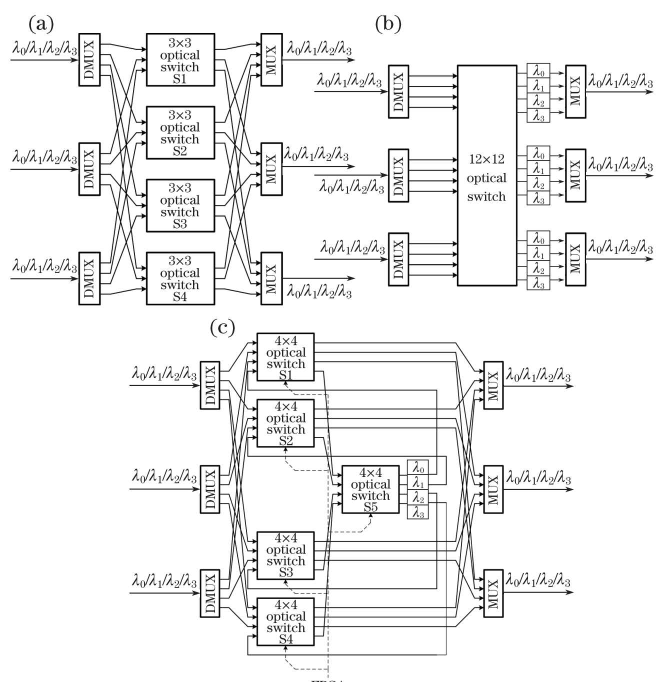

Fig. 1. Architectures of (a) WSXC, (b) WIXC, and (c) the devised L-WIXC. MUX: multiplexer; DMUX: demultiplexer.

module ahead of the offset time, prior to the corresponding BDPs. The frequency of the four DFB-LDs were f_1 = 191.6 THz, f_2 = 192.6 THz, f_3 = 193.6 THz, and f_4 = 194.6 THz, respectively. The average emissive power was –10 dBm. The FPGA control module was used to assign and reserve the available wavelengths according to the information carried by the BCP, including destination address, burst size, offset time, and resource reservation protocol (e.g., JIT and just-enough-time (JET))[9]. The optical switches were configured using the FPGA control module. However, once the FPGA control module was unable to reserve the wavelength for certain BCPs, the corresponding BDPs were discarded. The optical receiver module can measure the optical power, crosstalk, eye diagram, and linear Q factor of the received signals.

The FPGA control module plays an important role in wavelength switching in L-WIXC. Notations used in the description of the JIT-based control flow for L-WIXC by FPGA are as follows.

Let $Q_1[\lambda_{ij}]$ denote the current state of the reserved wavelengths in L-WIXC, and λ_{ij} be a Boolean variable, where i ($i = 0, 1, 2$) represents the number of the output ports and j ($j = 0, 1, 2, 3$) represents the wavelength number of the corresponding output ports. The wavelength j at output i is reserved when $\lambda_{ij} = 1$, whereas it is free when $\lambda_{ij} = 0$.

Let $Q_2[\mathrm{t}_{ij}]$ denote the reserved time when the corresponding wavelength is $Q_1[\lambda_{ij}]$. Here, t_{ij} is an integer variable. If $t_{ij} = 0$, then $\lambda_{ij} = 0$; otherwise, $\lambda_{ij} = 1$.

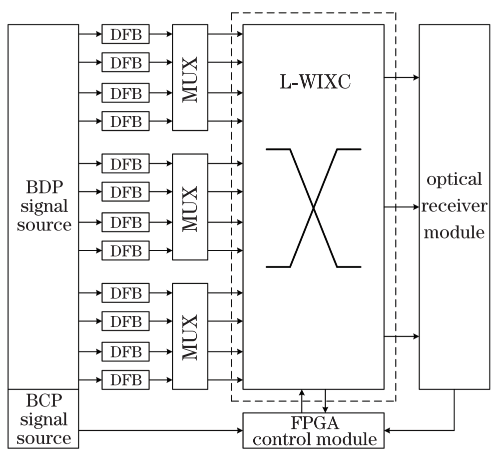

Fig. 2. Test bed for the devised L-WIXC.

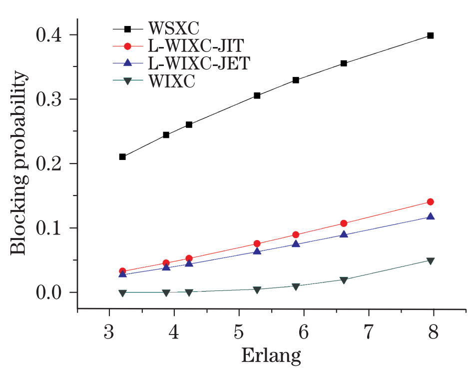

Fig. 3. Blocking probability comparison of WSXC, L-WIXC, and WIXC.

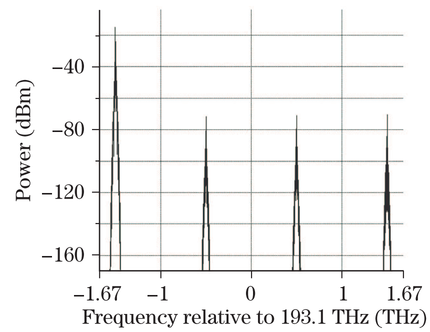

Fig. 4. Channel crosstalk without wavelength conversion.

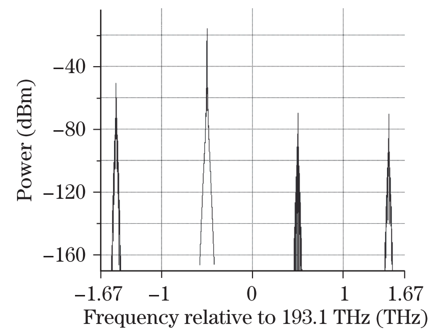

Fig. 5. Channel crosstalk with wavelength conversion.

Let BL(n) denote the burst length of BDP(n), and OT(n) denote the offset time of BDP(n). For a new arrival BCP(n), the procedures of the control algorithm that adopts the JIT protocol are as follows.

Step 1: Record the essential information carried by BCP(n), such as destination address i, input wavelength number j, BL(n), and OT(n).

Step 2: Search the matrix Q_1. If $\lambda_{ij} = 0$, then t_{ij} = BL(n) + OT(n) and $\lambda_{ij} = 1$. Then proceed to Step 4. If $\lambda_{ij} = 1$, proceed to Step 3.

Step 3: Check if $\lambda_{ik} = 0$ ($k = 0, 1, 2, 3$ and $k \neq j$), then transfer the input wavelength j to S5 and convert wavelength j to wavelength k. If t_{ik} = BL(n) + OT(n), λ_{ik} = 1, then proceed to Step 4; otherwise, discard the BCP.

Step 4: Update Q_1 and Q_2. Wait for the next BCP(n+1).

Let ρ denote the average burst arrival rate at input ports, $1/\mu$ denote the average burst length (duration), and W denote the wavelength number. Thus, the offered load is $r = \rho/\mu$. WSXC behaves as a W independent single server M/M/1/1 loss system (M/M/1/1 means single server queue with Poisson arrivals, exponetially distributed service times, and at most one customer in the queue), with $r = \rho/(\mu \times W)$. WIXC behaves as an M/M/W/W loss system, with $r = \rho/\mu$. L-WIXC can be formulated using a continuous-time Markov chain with a block tridiagonal infinitesimal generator[10]. The blocking probability of WSXC, WIXC, and the proposed L-WIXC is simulated. The results are shown in Fig. 3.

The maximum throughput of the devised L-WIXC was calculated. Assume that the BDP size ranges from 120 to 240 Mb, the transmitting rate is 10 Gb/s, and the offset time changes from 12 to 24 ms. When the blocking probability is 5%, the maximum throughput of the devised L-WIXC adopting JIT is 24 Gb/s, whereas that of the devised L-WIXC adopting JET is 31.9 Gb/s.

According to the market price of devices, the unit price of a 4×4 optical switch is 22500 RMB, that of multiplexer and demultiplexer is 1000 RMB, and that of WC is 5000 RMB. Hence, the cost of WSXC (Fig. 1(a)) is approximately 96000 RMB. Note that 3×3 optical switches in WSXC are replaced by 4×4 optical switches. Meanwhile, the cost of WIXC (Fig. 1(b)) is approximately 566000 RMB because the 12×12 optical switch it incorporates is expensive. The cost of the devised L-WIXC is approximately 138500 RMB. Therefore, the devised L-WIXC is a cost-effective solution when compared with WSXC and WIXC.

The optical parameters of the devised L-WIXC (i.e., channel crosstalk, eye diagram, and linear Q factor) were measured. A single mode fiber was used to connect the optical devices, and the key parameters of the fiber are as follows: attenuation is 0.2 dB/km; dispersion is 1.6×10^{-5} s/m^2; and the total fiber length changes from 10 to 50 km. The crosstalk of the optical switch is –30.0 dB. The simulation results of the optical parameters in the L-WIXC are as follows.

Figure 4 shows the simulation result of the channel crosstalk without wavelength conversion. The optical power at f_1 = 191.6 THz is approximately –15 dBm, which is lower than the original power (–10 dBm). Compared with the optical power of the other three frequencies (–70 dBm), the intensity of the chosen signal is much higher than that of the crosstalk. Therefore, the channel crosstalk barely has an effect on the chosen signal under the absence of wavelength conversion.

Figure 5 illustrates the simulation result of the channel crosstalk with wavelength conversion. The optical power at f_1 = 191.6 THz is approximately –15 dBm, which is lower than the original power (–10 dBm). Compared with the optical power of the other three frequencies (changes from –70 to –50 dBm), the intensity of the chosen signal remains much higher than that of the crosstalk. Thus, the channel crosstalk barely has an effect on the chosen signal under wavelength conversion.

Figures 6(a)–(c) show the eye diagrams when the fiber lengths are 15, 25, and 35 km, respectively. In Fig. 6(a), the inter-symbol interference is weak, whereas the eye diagram is clear. In Fig. 6(b), the quality of the eye diagram is degraded; however, the inter-symbol interference remains bearable. In Fig. 6(c), the eye diagram has become vague, whereas the inter-symbol interference continues to be too strong for the signals to transmit.

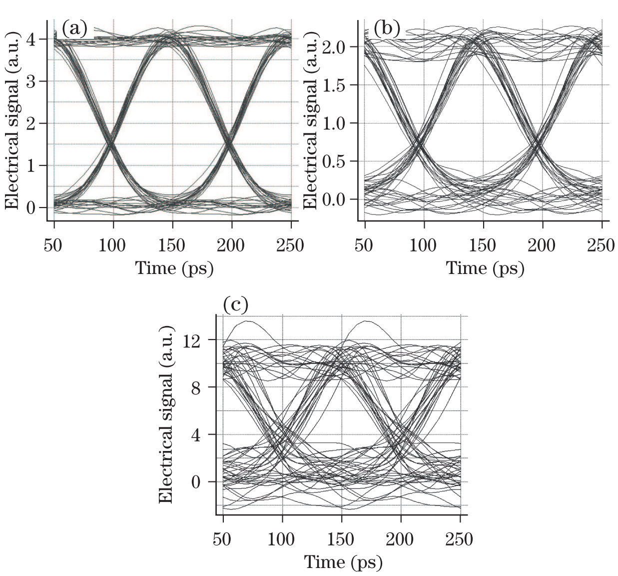

Fig. 6. Eye diagrams at (a) 15, (b) 25, and (c) 35 km.

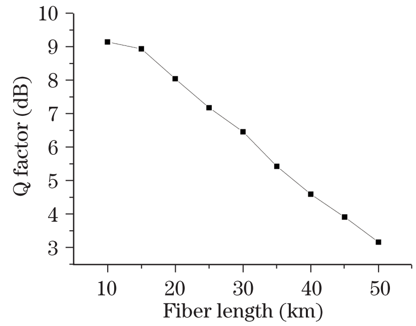

Fig. 7. Linear Q factor versus fiber length.

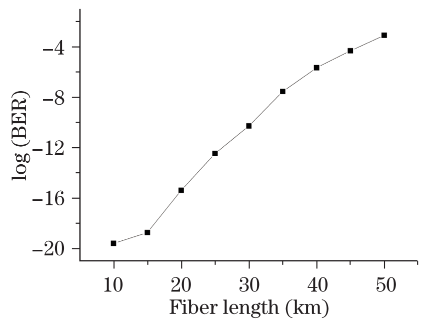

Fig. 8. BER versus fiber length.

The ultimate performance measure of the devised L-WIXC is its bit error rate (BER). However, performing the simulation is too time-consuming. BER is therefore estimated indirectly, usually by measuring the linear Q value of the system through assessing the sensitivity of a system to change the 1/0 detection threshold. The BER can be approximately related to Q by

$$\mathrm{BER} = \frac{1}{\mathrm{Q}\sqrt{2\pi}} \exp\left(-\frac{\mathrm{Q}^2}{2}\right). \tag{1}$$

The optical signal-to-noise ratio (OSNR) can be used as a first estimate of the linear Q value of the received bits. The following equation relates linear Q to OSNR:

$$\mathrm{Q} = \frac{2\times \mathrm{OSNR}\sqrt{\frac{B_\mathrm{o}}{B_\mathrm{e}}}}{1+\sqrt{1+4\times \mathrm{OSNR}}}, \tag{2}$$

where B_o is the optical bandwidth of the receiver and B_e is the electrical bandwidth of the receivers post-detection filter.

Figure 7 shows the simulation results of linear Q factor versus fiber length. Linear Q value declined from 9.1 to 3.2 dB when the fiber length increased from 10 to 50 km. The linear Q value was 6.0 dB when the fiber length was 32 km, which is the typical standard for most optical communication systems.

Figure 8 shows the simulation results of the BER versus fiber length. The BER declined from 1×10^{-20} to 1×10^{-3} when the fiber length increased from 10 to 50 km. The BER was 1×10^{-9} when the fiber length was 32 km.

In conclusion, the L-WIXC we have devised in this letter is a cost-effective solution for supporting OBS compared with WSXC and WIXC. The components adopted for the L-WIXC are mature and reliable, making it feasible and practical. Moreover, the simulation results of optical parameters show that L-WIXC meets the requirements of a wavelength division multiplexing (WDM) communication system with an effective transmission distance of 32 km when the average emissive power is –10 dBm.

This work was supported by the Natural Science Foundation of Zhejiang Province, China (No. Y1080172) and was a key industrial project for science and technology development of Zhejiang Province, China (No. 2009C11051).

References

1. G. S. Zervas, M. De Leenheer, L. Sadeghioon, D. Klonidis, Y. Qin, R. Nejabati, D. Simeonidou, C. Develder, B. Dhoedt, and P. Demeester, J. Opt. Commun. Netw. **1,** 69 (2009).
2. M. De Leenheer, C. Develder. J. Buysse, B. Dhoedt, and P. Demeester, Opt. Switch. Netw. **6,** 88 (2009).
3. P.-H. Ho, H. T. Mouftah, and J. Wu, IEEE J. Sel. Areas Commun. **21,** 1133 (2003).
4. T. Goh, T. Kitoh, M. Kohtoku, M. Ishii, T. Mizuno, and A. Kaneko, in *Proceedings of OFC/NFOEC 2008* OWC6 (2008).
5. X.-J. Kuo and C. Chen, in *Proceedings of 2007 IEEE Workshop on High Performance Switching and Routing* 126 (2007).
6. Y. Zhao, J. Zhang, D. Han, X. Zhang, Y. Yao, W. Gu, and Y. Ji, IET Commun. **3,** 1716 (2009).
7. W. Li, D. Liu, C. Yang, C. Wu, J. Zhu, X. Zhou, and M. Mao, Chinese J. Lasers (in Chinese) **33,** 351 (2006).
8. J. Comellas, J. Conesa, and G. Junyent, Photon. Network Commun. **5,** 81 (2003).
9. P. Hou, Z. Song, X. Li, J. Zhang, and L. Liu, Acta Opt. Sin. (in Chinese) **28,** 365 (2008).
10. N. Akar and E. Karasan, in *Proceedings of 1st International Conference on Broadband Networks* 110 (2004).